HACETTEPE JOURNAL OF BIOLOGY AND CHEMISTRY Research Article
Hacettepe J. Biol. & Chem., 2008, 36 (3), 247-253

PAN-Based Pd-doped Activated Carbon Fibers for Hydrogen Storage: Preparation, A new Method for Chemical Activation and Characterization of Fibers

Serkan Baş[1], Özgül Hakli[2], Ahu Gümrah Dumanli[1] and Yuda Yürüm[1]*

[1]Faculty of Engineering and Natural Sciences, Sabanci University, Tuzla, 34956 Istanbul, Turkey

[2]Department of Chemistry, Celal Bayar University, Muradiye, 45030 Manisa, Turkey

Abstract

The preparation of ACFs from PAN fibers under various conditions and the method to load Pd on ACFs were described. Chemical activation of the fibers increased the surface areas of the fibers from about 64 m^2/g to 381 m^2/g. SEM micrographs of Pd-loaded indicated the diameters of the fibers were in the range of 1.0-10.0 mm. Diameters of metallic Pd particles on the fibers changed between 80 nm and 100 nm. 4.5% (by wt) metallic palladium was deposited on the ACFs. This high percentage of palladium deposited on ACFs is useful for hydrogen storage, since Pd-H system is established under a wide range of pressure and temperature.

Key Words: Polyacrylonitrile fibers, activated carbon fibers, BET surface area, scanning electron microscopy.

INTRODUCTION

Hydrogen storage on carbon materials has recently been attracting interest because of the significance of hydrogen as an energy carrier in automotive products. In order to upgrade the hydrogen storage capacity of carbon materials, numerous techniques have been proposed [1–4].

Particularly carbon materials, such as activated carbon, carbon fibers, carbon nanotubes and carbon nanofibers have caught the attention of scientists of different disciplines. The mechanism of hydrogen storage and the interaction between the carbon surface and hydrogen are not sufficiently comprehended. Carbon materials adsorb hydrogen through physical interactions, and the binding energy between the solid and the H_2 molecule is extremely inadequate to accomplish noteworthy levels of adsorption at room temperature. Only at cryogenic temperatures the intensity of the interaction increases noticeably, and physical adsorption gives the hydrogen capacity that is required for storage [5]. In order to improve the hydrogen sorption capacity of carbon materials at room temperature, it is essential to raise the strength of the gas–solid interaction. Alternatively, the increase in the extent of the binding energy must be reasonable, because too strong interactions form

* Correspondence to: Yuda Yürüm,

Faculty of Engineering and Natural Sciences, Sabanci University, Tuzla, Istanbul 34956, Turkey
Tel: +90216 483 9512 Fax: +90216 483 9550
E-mail: yyurum@sabanciuniv.edu

irreversible bonds, as in the case of chemisorption. Evidently, an irreversible H_2 sorption avoids the use of the material for storage purposes since hydrogen must be straightforwardly desorbed from the storage system.

Oxygen functional groups have also been revealed to be a factor in physisorption of hydrogen on activated carbon: increasing oxidation functional groups of an activated carbon caused an increase in physisorption [6]. The outcome of surface functionalities on physisorption of hydrogen to carbon has not been extensively investigated, but hydrogen adsorption has been demonstrated to chemically alter functional groups on carbon to create basic carbons [7]. Without a doubt, the wide diversity of existing carbon structures gives a remarkable occasion to methodically clarify the effect of carbon properties, including pore size, graphitic content and surface functionalities, on hydrogen adsorption.

Recently, metal doping has drawn much interest as some selected metals increase hydrogen storage because of the formation of active spots on the carbon materials, improving hydrogen adsorption [8–11]. The interaction of noble metals, such as palladium and platinum with carbon nanotubes works as the prototypical transition metal–CNT interaction and for that reason, is one of the most examined systems [12-15]. In spite of this, the hydrogen storage capacities of such systems are inadequately understood, rationalizing their complexity.

Takagi et al. [16] described that the hydrogen storage capacities of Pt and Pd-doped activated carbon resulted from the sorption of hydrogen on metal and carbon phases, telling a simple cumulative effect. In some examples, the variation in the hydrogen storage capacities of metal doped carbon materials can be completely attributed to the size of metal particles involved [17]. Thus at this phase, additional experiments are essential, to provide more complete understanding of the metal-mediated hydrogen storage development in carbon nanotubes.

In the present report, we describe the structural characteristics of raw, surface-treated and palladium-doped carbon fibers. First, the carbon fibers were characterized in terms of physical and chemical properties in order to extend this information to hydrogen adsorption. Secondly, carbons were doped with palladium in an attempt to optimize a carbon-metal system and find a promising material for hydrogen storage goals. The palladium nanoparticles were doped on to carbon fibers via impregnation and in situ condensed phase reduction method. The preparation of CFs from PAN fibers under various conditions and the method to load Pd on ACFs was investigated. Structure of the CFs were explored by surface analysis, FTIR spectrometry and scanning electron microscopy (SEM) methods. The next paper in the series will report hydrogen storage measured at 298 K and a pressure range of 0.66–2.22 MPa, technically relevant for practical hydrogen storage applications.

EXPERIMENTAL

Production and chemical activation of CFs.

Commercial 1.1 decitex PAN fibers (weight of 10,000 m of single fiber in gram is 1 decitex) obtained from AKSA Acrylic Chemical Industries, Yalova, Turkey, were used in the present work. Fiber samples were stabilized, while it was stretched, for 48 hours under a static air atmosphere in an oven at 250°C. Stretching of the fibers prevented curling of the stabilized fibers. The stabilized fibers were carbonized at 1100°C for 3 hours under a nitrogen atmosphere. Carbonized fibers retained their fibrous structure and their color became black after

carbonization. A new method of chemical activation of carbon fibers is proposed in the present study. 1.6 g of carbon fibers (CF) were immersed into 30 mL, 0.3 M aqueous solution of $Al(OH)_3$ and stirred for 6 hours at room temperature. CFs separated by filtration were dried at room temperature and activated at 1100°C under an argon atmosphere for 3 hours. The probable activation reactions were as follow:

$$2\ Al(OH)_3 \rightarrow Al_2O_3 + 3\ H_2O \quad (1)$$

$$2\ Al_2O_3 + 3\ C \rightarrow 3\ CO_2 + 4\ Al \quad (2)$$

$$CO_2 + C \rightarrow 2\ CO \quad (3)$$

Reactions (2) and (3) are the reactions that CFs lost carbon material and the surface of the fibers thus lost original smoothness by the creation of new porosity. Aluminum residues that attached on the surface of activated carbon fibers (ACFs) were dissolved by stirring the fibers in 10% nitric acid for 2 hours, then the fibers were rinsed thoroughly with water and dried at 100°C in an oven.

Doping of ACFs with Pd.

0.5 g of ACFs was stirred with 50 ml of aqueous hydrazine solution (hydrazine:water = 1:200, by volume) for 10 hours (Solution 1). 0.0417 g $PdCl_2$ (Aldrich, 99.999 %) was dissolved in 20 mL KOH:NH_4OH (by wt) solution at room temperature (Solution 2). Solution 1 was added to the Solution 2 as reducing agent for Pd^{2+}. Metallic Pd appeared on the surface of ACFs after several hours of reaction time. The Pd-doped-ACFs were then washed with distilled water to clean the ACFs from the residual matter and organics, and dried in an oven at 70°C under a nitrogen atmosphere. Washing of the fibers with fresh distilled water leached negligible amounts of metallic Pd particles.

Surface analysis.

Surface areas of CFs, ACFs were measured by Quantachrome NOVA 2200e series Surface Analyzer. The determination is based on the measurements of the adsorption isotherms of nitrogen at 77 K. Surface area of the samples were determined by using BET equation in the relative pressure range of between 0.05 to 0.3, seven adsorption points and BJH (Barrett-Joyner-Halenda) method was utilized for the measurement of pore size distributions. Before all of the measurements, moisture and gases such as nitrogen and oxygen adsorbed on the surface or held in the open pores, were removed under reduced pressure at 100°C for 5 h.

FTIR spectrometry.

FT-IR spectra of CFs, ACFs and Pd-doped-ACFs were measured with a Bruker EQUINOX 55 FT-IR spectrometer. Activated carbon samples were dried under a nitrogen atmosphere at 110°C for 24 hours. KBr pellets were prepared by grinding 2.5 mg of dry sample with 200 mg of dried KBr. Spectra were obtained with 200 scans at a resolution 2 cm^{-1}. The assignment of the bands in the infrared spectra was according to early reports [18,19].

SEM analysis.

The CFs, ACFs and Pd-doped-ACFs were examined with a Leo G34-Supra 35VP scanning electron microscope. Imaging was generally done at 2-5 keV accelerating voltage, using the secondary electron imaging technique.

RESULTS AND DISCUSSION

FTIR spectra of carbon fibers.

The FTIR spectra of carbon fibers stabilized at 250°C for 1 hour and carbonized for 1 hour at 600°C, 700°C, 800°C and 1100°C are presented in Figure 1. All of the spectra were similar, the main difference was the low intensity bands due to nitrogen and oxygen functional groups as the carbonization temperature was increased to 1100°C indicating that

more carbonaceous material was formed at higher temperatures. The major bands observed in the FTIR spectra were the following: weak bands near 3655 cm^{-1} of free –O–H stretching vibrations due to probably humidity adsorbed during measurements; twin peaks at 2982 cm^{-1} and 2891 cm^{-1} due to symmetric stretching vibrations of $–CH_2$ and stretching vibrations of –CH, respectively. The intensity of these twin peaks decreased as the carbonization temperature was increased to 1100°C. The strong bands at 1564 cm^{-1} were due to –N–H bending and –C–N= vibrations. The intensity of these functionalities also decreased very sharply as the carbonization temperature was increased to 1100°C. As a matter of fact in the FTIR spectrum of the sample produced at 1100°C it is quite impossible to observe these bands. The same is true for the bands at 1400 cm^{-1} of –N–N=O asymmetric stretching and –O–H bending vibrations and for the bands at 1254 cm^{-1} due to –C–N– stretch and $–CH_3$ rocking vibrations. The bands at 1164 cm^{-1}, at 1090 cm^{-1} and at 964 cm^{-1} were as a result of $–CH_3$ rocking, –C–OH stretching and –C=C–H out-of-plane C–H vibrations, respectively.

Structural characteristics of the ACFs.

The SEM micrographs of carbon fibers stabilized at 250°C and carbonized at 1100°C for 1 hour are presented in Figure 2. The shape of the fibers was cylindrical as they were before the carbonization experiments. Fibers of non-uniform shape were produced after stabilization and carbonization experiments. It seemed that some of the fibers sticked to each other due to softening of the fibers during the thermal treatment. Surface of the fibers was observed to contain some roughness due to activation reactions which volatilized some of the carbon material from the surface of the fibers and activation of the fibers caused some material loss from the surface creating irregular channels on the surface, Figure 3. An additional feature in the SEM of the fibers in Figure 3 was the presence of aluminum residues. These were removed after nitric acid treatment.

The BET surface areas measured before activation were in the range of 64-75 m^2/g. Activation of the fibers increased the surface areas of the fibers to 381 m^2/g. ACFs show higher apparent specific

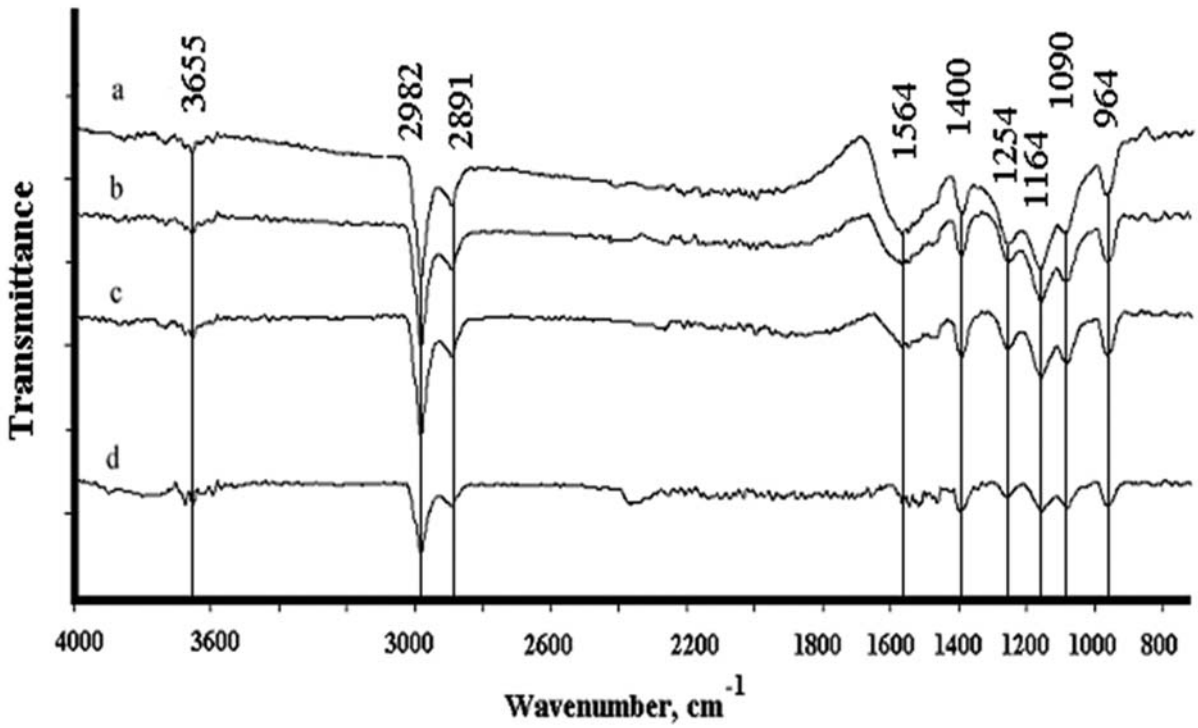

Figure 1. FTIR spectra carbon fibers stabilized at 250°C for 1 hour and carbonized for 1 hour at a) 600°C, b) 700°C, c) 800°C and d) 1100°C.

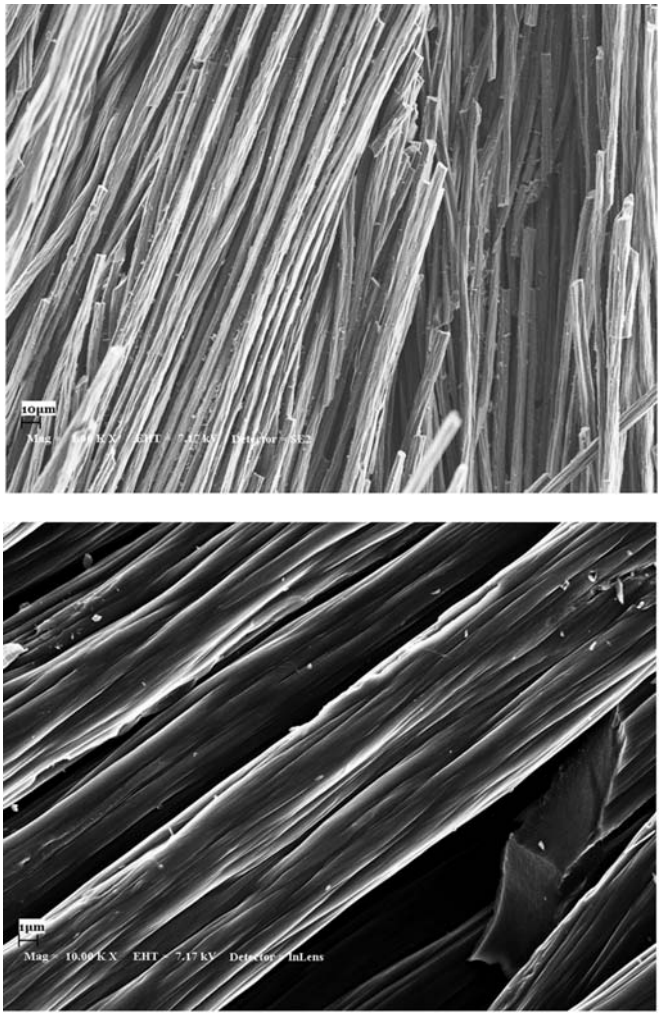

Figure 2. SEM micrographs of PAN fibers carbonized at 1100°C before activation.
Top figure, magnification = 1.00 KX, bottom figure, magnification = 10.00 KX.

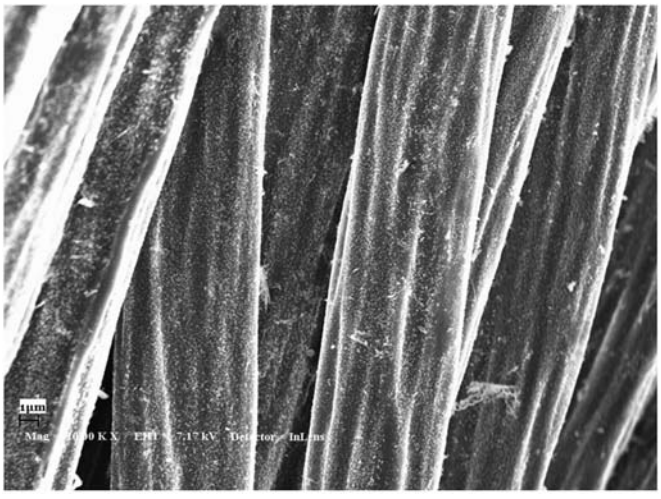

Figure 3. SEM micrographs of carbon fibers after chemical activation, before aluminum deposition was washed with nitric acid treatment. Top figure, magnification = 1.00 KX, bottom figure, magnification = 10.00 KX.

surface areas normally in the range of 1500–3000 m^2/g, The BET areas measured in the present work were much lower than these values. The reason for this was probably the new chemical method proposed in the present work was a milder method when compared with the other chemical activation methods. The pore size distribution of the ACFs are presented in Figure 4. The ACFs contained pores with diameters of 2-5 nm, therefore the porosity of the fibers can be considered as mesoporous since types of pores as defined by IUPAC are microporous with width not exceeding 2 nm, mesoporous with width between 2 nm and 50 nm and macroporous with width exceeding 50 nm [20].

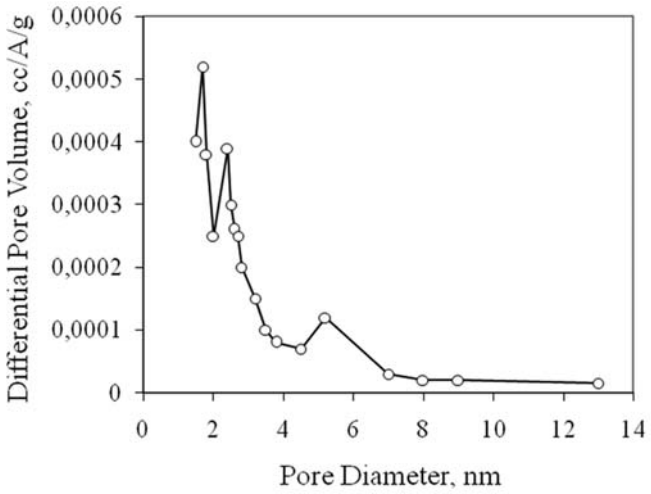

Figure 4. BJH pore distribution graph of ACFs.

Pd-loaded ACFs.

SEM micrographs of Pd-loaded ACFs are presented in Figure 5. While diameters of the fibers were measured as 0.5-1.0 μm, the diameters of metallic Pd particles loaded on the fibers changed approximately between 80 nm and 100 nm. The shape of the Pd particles seemed to be spherical on the average though some non-spherical Pd particles also existed on the fibers. The diameters of the Pd particles formed in the present study were greater than those reported by Bulushev et al [21]. Gold nanoparticles of 2–5 nm diameters formed on woven fabrics of ACFs. To form highly dispersed 0.8 % (by wt.) Au nanoparticles, gold was deposited on

activated carbon fibers (ACF) from $[Au(en)_2]Cl_3$ solution. The reason for this difference was the utilization of a different method for the deposition of the Pd^0. The percentage of the Pd^0 deposited on carbon fibers was 4.5 % (by wt), this value was much greater than that of the value in Bulushev et al. [21]. This high percentage of palladium deposited on ACFs is useful for hydrogen storage, since Pd-H system is established under a wide range of pressure and temperature [22].

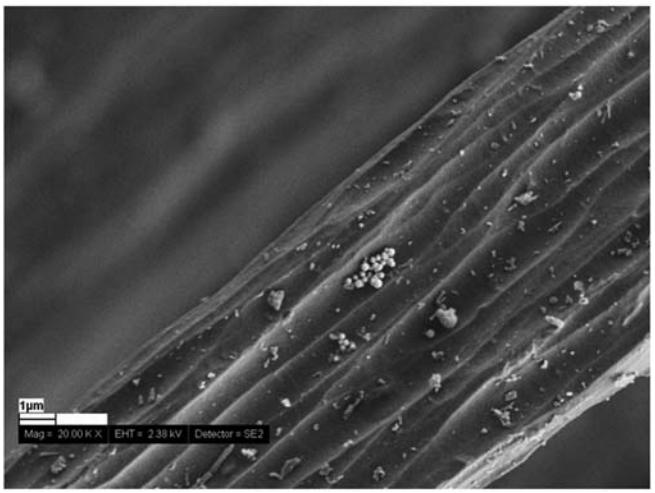

Figure 5. SEM micrographs of ACFs after Pd doping. Magnification = 20.00 KX.

CONCLUSIONS

The BET surface areas before activation were in the range of 64-75 m^2/g. Activation of the fibers with carbon dioxide increased the surface areas of the fibers to about 381 m^2/g. The ACFs contained pores with diameters of 2-5 nm, therefore the porosity of the fibers can be considered as mesoporous. It seemed that chemical activation process proposed was not very efficient in producing high surface area fibers under the conditions applied in the present study.

The major bands observed in the FTIR spectra were weak bands near 3655 cm^{-1} of free –O–H stretching vibrations due to probably humidity adsorbed during measurements; twin peaks at 2982 cm^{-1} and 2891 cm^{-1} due to symmetric stretching vibrations of $–CH_2$ and stretching vibrations of –CH, respectively. The strong bands at 1564 cm^{-1} were due to –N–H bending and –C–N= vibrations. The intensity of these functionalities decreased very sharply as the carbonization temperature was increased to 1100°C, as a matter of fact in the FTIR spectrum of the sample produced at 1100°C it is quite impossible to observe these bands.

SEM micrographs of Pd-loaded indicated the diameters of the fibers were in the range of 0.5-1.0 µm. Diameters of metallic Pd particles loaded on the fibers changed approximately between 80 nm and 100 nm. The shape of the Pd particles seemed to be spherical on the average though some non-spherical Pd particles also existed on the fibers. 4.5% (by wt) metallic palladium was deposited on the ACFs.

REFERENCES

1. A. C. Dillon, K. E. H. Gilbert, J. L. Alleman, T. Gennett, K. M. Jones, P. A. Parilla, M. J. Heben, in: Proceedings of the 2001 DOE Hydrogen Program Review, NREL/ CP-570-30535, 2001.
2. E. David, J. Mater. Proc. Technol. 162/163 (2005) 169.
3. G. G. Tibbetts, G. P. Meisner, C. H. Olk, Carbon 39 (2001) 292.
4. H. M. Cheng, Q. H. Yang, C. Liu, Carbon 39 (2001) 1447.
5. L. Zhou, Y. Zhou, Y. Sun, Int. J. Hydrogen Energy 29 (3) (2004) 319.
6. R. K. Agarwal, J. S. Noh, J. A. Schwarz, P. Davini, Carbon 25 (1987) 219.
7. J. A. Menendez, L. R. Radovic, B. Xia, J. Phillips, J. Phys. Chem. 100 (1996) 17243.

8. P. Chen, X. Wu, J. Lin, K. L. Tan, Science 285 (1999) 91.

9. Z. H. Zhu, G. Q. Lu, S. C. Smith, Carbon 42 (2004) 2509.

10. S. Challet, P. Azais, R. J.-M. Pellenq, O. Isnard, J. -L. Soubeyroux, L. Duclaux, J. Phys. Chem. Solids 65 (2004) 541.

11. K. Kim, H. Lee, K. Han, J. Kim, M. Song, M. Park, J. Lee, J. Kang, J. Phys. Chem. B 109 (2005) 8983.

12. S. Dag, Y. Ozturk, S. Ciraci, T. Yildirim, Phys. Rev. B 72 (2005) 155404.

13. A. Lueking, R.T. Yang, J. Catal. 206 (2002) 165.

14. F.H. Yang, A.J. Lachawiec, R.T. Yang, J. Phys. Chem. B 110 (2006) 6236.

15. A. Anson, E. Lafuente, E. Urriolabeitia, R. Navarro, A.M. Benito, W. K. Maser, M.T. Martinez, J. Phys. Chem. B 110 (2006) 6643.

16. H. Takagi, H. Hatori, Y. Yamada, S. Matsuo, M. Shiraishi, J. Alloy. Compd. 385 (2004) 257.

17. J. Ozaki, W. Ohizumi, A. Oya, M. J. Illan-Gomez, M. C. Roman- Martinez, A. Linares-Solano, Carbon 38 (2000) 775.

18. G. Shevla, G. Comprehensive Analytical Chemistry, Volume VI, Analytical Infrared Spectroscopy, Elsevier, Amsterdam, 1976, pp. 334.

19. Y. Yürüm, N. Altuntas, Fuel Science and Technol. Int., 12 (1994) 1115.

20. IUPAC Compendium of Chemical Terminology, second ed., vol. 46, 1997, p. 1976.

21. D. A. Bulushev, I. Yuranov, E. I. Suvorova, P. A. Buffat, L. Kiwi-Minsker, J. Catalysis, 224 (2004) 8.

22. G. Sandrock, Hydrogen-Metal Systems, in Hydrogen Energy System, Y. Yürüm (Ed.), NATO ASI Series E, Vol. 295, Kluwer Academic Publishers, Dordrecht, 1995, pp. 135.